

PID Control Tuning Based on Wind Speed Sensor in Flying Robot

Fadlur Rahman T. Hasan¹, Son Ali Akbar^{2,*}

^{1,2}Department of Electrical Engineering, Universitas Ahmad Dahlan, Yogyakarta, Indonesia

Email: ¹fadlur1600022047@webmail.uad.ac.id, ²sonali@ee.uad.ac.id

*Corresponding Author

Abstract—The problem that is often faced by flying robots when carrying out the Vertical Take Off Landing (VTOL) process is the lack of stability of the vehicle due to differences in wind speed at any time. This is because the PID that has been pre-tuned is the PID at a certain wind speed and it is possible that during the race the wind speed suddenly changes, causing the vehicle to be less stable in carrying out the mission. Therefore, this study proposes a PID Control Tuning Control system based on the Wind Speed Sensor. In experiments that have been carried out with anemometer readings of 1-5 m/s, the ideal tuning results are obtained with each parameter $P_{roll} = 0.1453$, $I_{roll} = 0.0892$, $D_{roll} = 0.004$, $P_{pitch} = 0.144$, $I_{pitch} = 0.09$, $D_{pitch} = 0.004$, $P_{yaw} = 0.184$, $I_{yaw} = 0.0184$, $D_{yaw} = 0.00309$. In experiments with anemometer readings of 6-10 m/s, the ideal tuning results were obtained with each parameter $P_{roll} = 0.148$, $I_{roll} = 0.0905$, $D_{roll} = 0.004$, $P_{pitch} = 0.1444$, $I_{pitch} = 0.09$, $D_{pitch} = 0.004$, $P_{yaw} = 0.1867$, $I_{yaw} = 0.0181$, $D_{yaw} = 0.0037$. In an experiment with an anemometer reading of 11-15 m/s, the ideal tuning results were obtained with each parameter $P_{roll} = 0.1494$, $I_{roll} = 0.09$, $D_{roll} = 0.004$, $P_{pitch} = 0.1457$, $I_{pitch} = 0.0902$, $D_{pitch} = 0.004$, $P_{yaw} = 0.1894$, $I_{yaw} = 0.018$, $D_{yaw} = 0.0037$. PID adjustment based on this anemometer sensor utilizes the latest real-time wind speed data to support the robot in order to overcome instability in certain wind conditions by tuning PID so that the vehicle can maintain stability when carrying out certain missions.

Keywords—KRTI, VTOL, PID, Anemometer, Tuning, Flying Robot

I. INTRODUCTION

The Indonesian Flying Robot Contest has several divisions, one of which is Vertical Take Off Landing (VTOL) with the mission of Pick and Drop Survival Kits. This division is contested with each team getting a chance to fly its vehicle fully autonomously in a predetermined area or arena [1], in which there are two survival kits locations. Its missions include flying to find payloads of survival kits, then sending them to a predetermined location. After that, the vehicle must also send logistics that have been loaded before take-off to be dropped to a predetermined place, and ends with landing to the initial position (HOME).

In its development, the technology used in flying robots still needs to be improved, one of which is the ability to maintain the stability of the vehicle in various wind speed conditions, where at this time flying robots still rely on trial and error in stabilizing the vehicle so that the authors consider this to be less efficient. in terms of time and energy. This is because when there is a change in wind speed, we need to do

trial and error again to get a state where the vehicle can be said to be stable.

There are indications that show poor performance on systems that have erratic outputs, time delays and are not linear [2] so that PID parameter tuning is deemed necessary to get the desired response. Over the past few years various PID tuning methods have been carried out, both linear and non-linear schemes [3]. In general, tuning done on the PID control system of the robot, both ground robots and unmanned vehicles is still manually tuning, namely by trying the parameter values of the PID starting from the lowest value until the PID control response value is found to be good. Regarding the application of proportional integral derivative control to the control of a balance robot that develops noise reduction using PID and Kalman-filter methods [4].

In this study [5] implemented a quadcopter to clean the glass windows of high-rise buildings with a manual PID tuning control process to maintain the stability of the height and position of the quadcopter. Meanwhile, research on modeling a hexacopter is carried out using the Newton-Euler method, namely by analyzing the forces acting on the hexacopter [6]. The parameters resulting from the equation calculation of the method are then checked by simulating the model. The stabilization of the hexacopter model utilizes a proportional derivative controller. This is because there is no control that is functional and simple from controlling the PID itself [7].

II. METHOD

Hardware design where in this section all robot frameworks are made by taking into account CoG and also the layout of the hardware that will be placed in the robot. The system design is presented in the form of a block diagram in Fig. 1.

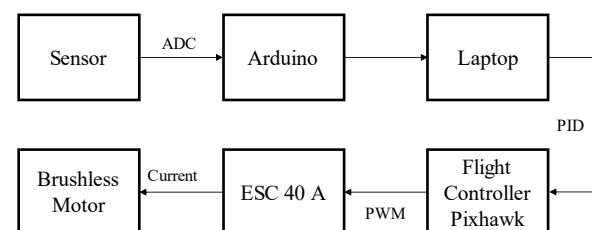


Fig. 1. Vehicle system block diagram

Drone API is communicated with multirotor using MAVLink (Micro Air Vehicle Link) MAVLink is a flight protocol used to communicate between GCS (Ground Control System) [8]. open source [9]-[10] and uses the Python programming language which is considered easy to

learn and the programming code is clear and easy to understand [11].

Fig. 2 and Fig. 3 is a flowchart or program flow or working process of the PID Adjustment Based on the JI-FS2 Anemometer Sensor.

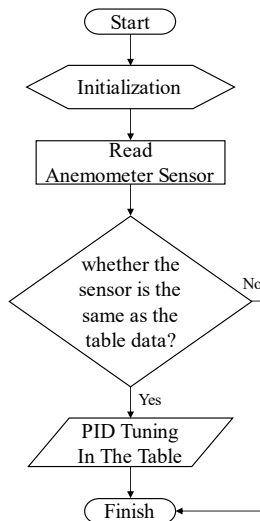


Fig. 2. System Flowchart

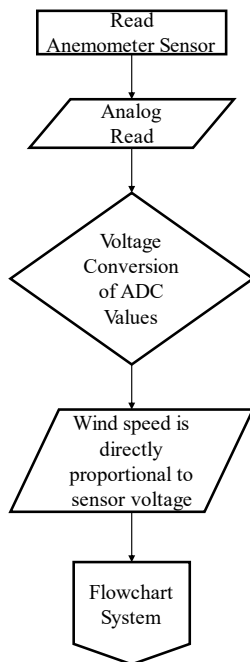


Fig. 3. Anemometer reading flow chart

Fig. 2 is a system flow diagram, the program first initializes then reads the anemometer sensor value as shown in Fig. 3, after that the value from the sensor will be read and compared with the data that has been taken previously. Then the value is matched with the collected reference data. then the data that matches a certain PID and then the program will execute according to the similarity with the data base. The event is in a loop or continues to repeat until the device is turned off. Indicated by the tool on which indicates when the tool is turned on, the program will be executed continuously, not just one cycle.

III. RESULT AND DISCUSSION

A. System Test

System testing is carried out to ensure that the system that has been created is in accordance with what is expected by the researcher. Stages of system testing begins in several stages as follows.

1) Brushless Motor Test

Before carrying out the test, it must be ensured that the (+) and (-) power cables and the ESC signal have been installed on the Pixhawk main output pin in accordance with the motor number sequence according to the type of frame used, in this study a hexa (+) frame type was used as shown in Fig. 4.

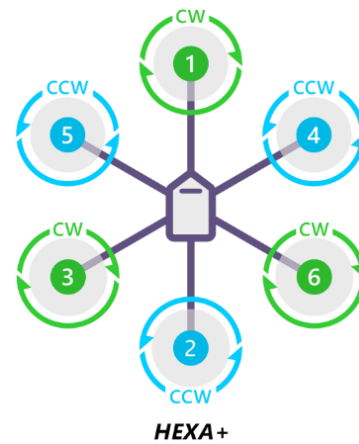


Fig. 4. Numbering order and direction of rotation

In Fig. 4 [12] the numbers indicate which output pins should be connected to each brushless motor. While the direction is shown in green for clockwise rotation (Clockwise, CW) and blue counterclockwise (Counter Clockwise, CCW). Next recognize the propeller clockwise and counterclockwise.

Fig. 5 shows the two types of propellers clockwise (called thrusters) and counterclockwise (called pullers). Then it is mounted on a brushless motor according to the direction of rotation of the motor [13]. Next check the motor numbering with the Mission Planner Motor Test Menu [12] which is shown in Fig. 6.

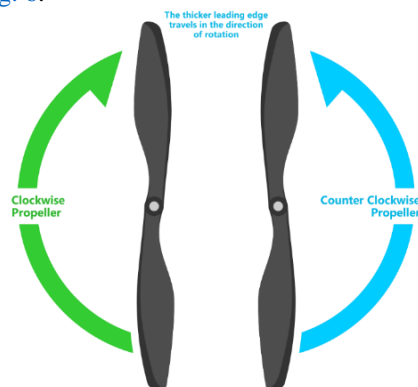


Fig. 5. Propeller turning direction

When connected via MAVlink, a test can be performed by clicking on the green button shown above and the corresponding motor will run for five seconds. Before carrying out the test make sure that the propeller is not

attached to the motor, if there is no motor turning, increase the throttle to 10% and try again. If it doesn't work, increase it to 15%.



Fig. 6. Motor Test

2) ESC Test

Most ESCs need to be calibrated so that the hardware can know the minimum and maximum PWM values that will be sent by flight control [14]. The thing that needs to be done before calibration is a safety check, where before taking action we need to make sure that the vehicle is not attached to the propeller and the flight control is not connected to the computer/laptop via USB and is not connected to the battery.

3) Tuning PID in Mission Planner

3DR IRIS works on various firmware. In this study working on copter hexa firmware [15]-[17]. To get optimal performance we may need to adjust the Mission Planner's Config/Tuning Copter Pids screen. Screenshot Fig. 7 shows the most important parameters for Roll/Pitch (yellow), Yaw (orange), Altitude hold (green), Loiter (pink) and Waypoint navigation (blue).

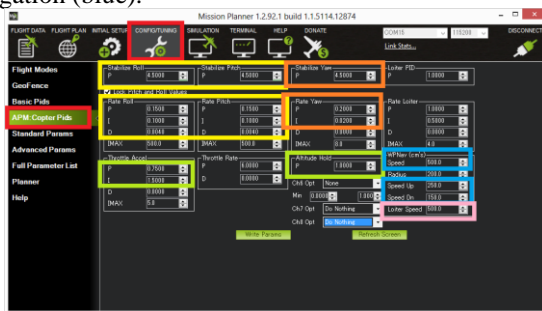


Fig. 7. Config/Tuning menu

In this study, data was collected which will later be used as comparison reference data in the PID adjustment process from the readable sensor itself. Data were collected from PID tuning from wind speeds of 5-15 m/s. The data collection process was carried out in sunny weather conditions. The value observed here is the ADC value of each change in wind speed with the PID tuning value. Relationship between wind speed and output voltage can be seen in Table 1. The tools used in the research can be seen in Fig. 8, Fig. 9, Fig. 10.

As information obtained from the datasheet that the relationship between wind speed and output voltage is

directly proportional, so the higher the wind speed, the higher the voltage read with changes in wind speed for each increase or decrease of 0.16-0.17 Volts. This has been proven through a graph plotter from the anemometer sensor readings in Fig. 11, Fig. 12, and Fig. 13.



Fig. 8. Hexacopter flying robot



Fig. 9. Wind speed sensor



Fig. 10. Wind speed reading on LCD display, Tegangan (Voltage)

Table 1. Relationship between wind speed and output voltage

| Wind Speed (m/s) | Voltage (V) | Wind Speed (m/s) | Voltage (V) |
|------------------|-------------|------------------|-------------|
| 1 | 0.17 | 16 | 2.67 |
| 2 | 0.33 | 17 | 2.83 |
| 3 | 0.5 | 18 | 3 |
| 4 | 0.67 | 19 | 3.17 |
| 5 | 0.83 | 20 | 3.33 |
| 6 | 1 | 21 | 3.6 |
| 7 | 1.17 | 22 | 3.67 |
| 8 | 1.33 | 23 | 3.83 |
| 9 | 1.5 | 24 | 4 |
| 10 | 1.67 | 25 | 4.17 |
| 11 | 1.83 | 26 | 4.33 |
| 12 | 2 | 27 | 4.5 |
| 13 | 2.17 | 28 | 4.67 |
| 14 | 2.33 | 29 | 4.83 |
| 15 | 2.5 | 30 | 5 |

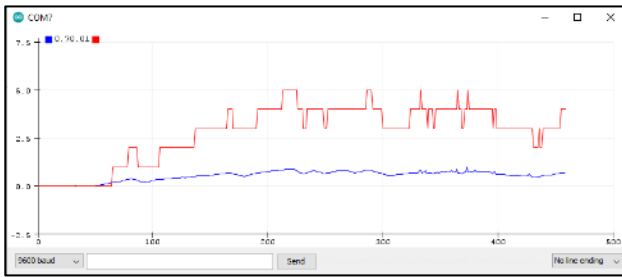


Fig. 11. The relationship between wind speed and output voltage wind speed 1-5 m/s

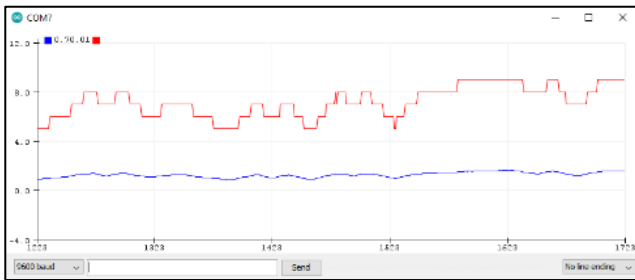


Fig. 12. The relationship between wind speed and output voltage wind speed 6-10 m/s

V_{out} data is obtained by measuring the measured sensor ADC value with the following equation:

$$V_{out} = SensorValue \times \frac{5}{1023} \quad (1)$$

where (1) will be used for all wind speed extraction.

After knowing the value of the sensor and the condition of the sensor, then data is taken for later determination of the program in the PID adjustment process based on wind speed.

Data retrieval by manually flying the drone is then carried out PID tuning based on the wind speed that is read at the same time then the value of each sensor will be observed by comparing it to the PID tuning which is then observed and found the character of each PID change based on wind speed. The results of taking these values are presented and then used as a reference during the programming process and form the output [18].

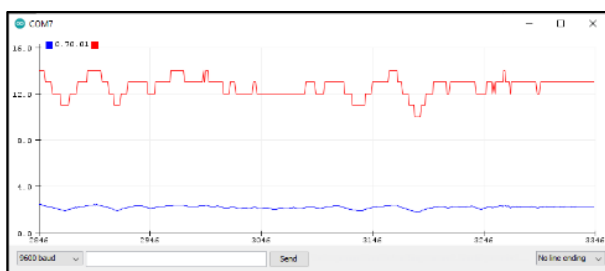


Fig. 13. The relationship between wind speed and output voltage wind speed 11-15 m/s

B. Extraction Wind Speed 1-5 m/s

After taking ten PID tuning data at wind speeds of 1-5 m/s, then using the average equation formula, the ideal PID tuning results are presented in Table 2.

From the results of observations and testing of the average PID of each extraction wind speed of 1-5 m/s, the degrees of pitch and roll are obtained in Table 3 and Fig. 14.

Table 2. Average extraction wind speed 1-5m/s

| | Average |
|--------|---------|
| Proll | 0.1453 |
| Iroll | 0.0892 |
| Droll | 0.004 |
| Ppitch | 0.144 |
| Ipitch | 0.09 |
| Dpitch | 0.004 |
| Pyaw | 0.184 |
| Iyaw | 0.0184 |
| Dyaw | 0.00309 |

Table 3. Degree of pitch and roll at wind speed 1-5 m/s

| ROLL (Degree) | PITCH (Degree) |
|---------------|----------------|
| 0.71 | -0.52 |
| 0.41 | -2.43 |
| 0.69 | -3.25 |
| 0.26 | -2.77 |
| -0.61 | 0.73 |
| -0.12 | -1.39 |
| 0.54 | -3.91 |
| -0.37 | -2.27 |
| 1.46 | -1.85 |
| -1.01 | -1.53 |



Fig. 14. Degrees of pitch and roll at wind speeds of 1-5 m/s

C. Extraction Wind Speed 6-10 m/s

After taking ten PID tuning data at wind speeds of 6-10 m/s then using the average equation formula, the ideal PID tuning results are presented in Table 4.

From the results of observations and testing of the average PID of each extraction wind speed 6-10 m/s obtained degrees of pitch and roll in Table 5 and Fig. 15.

Table 4. Average extraction of wind speed 6-10 m/s

| | Average |
|--------|---------|
| Proll | 0.148 |
| Iroll | 0.0905 |
| Droll | 0.004 |
| Ppitch | 0.1444 |
| Ipitch | 0.09 |
| Dpitch | 0.004 |
| Pyaw | 0.1867 |
| Iyaw | 0.0181 |
| Dyaw | 0.0037 |



Fig. 15. Degrees of pitch and roll at wind speeds of 6-10 m/s

Table 5. Degree of pitch and roll at wind speed 6-10 m/s

| ROLL (Degree) | PITCH (Degree) |
|------------------|-------------------|
| -0.78 | 0.68 |
| 0.42 | 2.18 |
| 0.24 | 2.76 |
| 6.04 | 3.51 |
| 1.68 | 0.55 |
| 3.16 | -1.2 |
| 3.53 | 3.84 |
| 1.45 | 1.53 |
| 2.9 | 2.67 |
| 1.25 | 2.07 |

D. Extraction Wind Speed 11-15 m/s

After taking ten PID tuning data at wind speeds of 11-15 m/s then using the average equation formula, the ideal PID tuning results are presented in Table 6.

From the results of observations and testing the average PID of each extraction wind speed 11-15 m/s obtained degrees of pitch and roll in Table 7 and Fig. 16.

Table 6. Average extraction wind speed 11-15 m/s

| | Average |
|--------|---------|
| Proll | 0.1494 |
| Iroll | 0.09 |
| Droll | 0.004 |
| Ppitch | 0.1457 |
| Ipitch | 0.0902 |
| Dpitch | 0.004 |
| Pyaw | 0.1894 |
| Iyaw | 0.018 |
| Dyaw | 0.0037 |

Table 7. Degree of pitch and roll at wind speed 11-15 m/s

| ROLL (Degree) | PITCH (Degree) |
|------------------|-------------------|
| 0.3 | -1.65 |
| 1.21 | -8.08 |
| 0.12 | -6.03 |
| 4.47 | -0.77 |
| 0.52 | -3.13 |
| 3.45 | -1.63 |
| -0.47 | -5.77 |
| 3.07 | -3.65 |
| -1.76 | -1.61 |
| 4.62 | -4.47 |



Fig. 16. Degree of pitch and roll at wind speed 11-15 m/s

IV. CONCLUSIONS

After conducting research and discussion, it has succeeded in building a PID Control Tuning system based on the Wind Speed Sensor. The test results of the JL-FS2 anemometer sensor for wind speed show an increase in the output voltage of 0.16 – 0.17 Volt, a change in wind speed of 1 m/s occurs [19]-[20].

In experiments with anemometer readings of 1-5 m/s, the ideal tuning results were obtained with each parameter Proll = 0.1453, Iroll = 0.0892, Droll = 0.004, Ppitch = 0.144, Ipitch = 0.09, Dpitch = 0.004, Pyaw = 0.184, Iyaw = 0.0184, Dyaw = 0.00309. While in the experiment with anemometer readings of 6-10 m/s, the ideal tuning results were obtained with each parameter Proll = 0.148, Iroll = 0.0905, Droll = 0.004, Ppitch = 0.1444, Ipitch = 0.09, Dpitch = 0.004, Pyaw = 0.1867, Iyaw = 0.0181, Dyaw = 0.0037. And experiments with anemometer readings of 11-15 m/s obtained ideal tuning results with each parameter Proll = 0.1494, Iroll = 0.09, Droll = 0.004, Ppitch = 0.1457, Ipitch = 0.0902, Dpitch = 0.004, Pyaw = 0.1894, Iyaw = 0.018, Dyaw = 0.0037.

From the information in the average tuning table and the pitch and roll degrees of each wind speed extraction, it was observed that the vehicle was stable because the tilt angle formed during this tuning average was applied, there was no slope that exceeded $\pm 5^\circ$ which was considered to be dangerous in carrying out a mission because it could cause crashes.

ACKNOWLEDGEMENT

The author would like to thank the academic community of Electrical Engineering Ahmad Dahlan University who have directly or indirectly provided input and views to the author to improve the quality of the writing to be published so that it is worthy of publication.

REFERENCES

- [1] S. J. Haddadi, P. Zarafshan, M. Dehghani, "A coaxial quadrotor flying robot: Design, analysis and control implementation," *Aerospace Science and Technology*, vol. 120, p. 107260, 2022, <https://doi.org/10.1016/j.ast.2021.107260>.
- [2] X. U. Wenfu, P. A. N. Erzhen, L. I. U. Juntao, L. I. Yihong, Y. U. A. N. Han, "Flight control of a large-scale flapping-wing flying robotic bird: System development and flight experiment," *Chinese Journal of Aeronautics*, vol. 35, no. 2, pp. 235-249, 2022, <https://doi.org/10.1016/j.cja.2021.03.009>.
- [3] C. B. Jabeur, H. Seddik, "Optimized neural networks-PID controller with wind rejection strategy for a Quad-Rotor," *Journal of Robotics and Control (JRC)*, vol. 3, no. 1, pp. 62-72, 2022, <https://doi.org/10.18196/jrc.v3i1.11660>.
- [4] B. Zhang, S. Furukawa and H. Lim, "Study on Automatic PID Gain Adjustment for a Four-rotor Flying Robot using Neural Network," *2019 4th Asia-Pacific Conference on Intelligent Robot Systems (ACIRS)*, pp. 104-108, 2019, <https://doi.org/10.1109/ACIRS.2019.8936012>.
- [5] J. Michalski, M. Retinger, P. Koziarski and W. Giernacki, "Position Control of Crazyflie 2.1 Quadrotor UAV Based on Active Disturbance Rejection Control," *2023 International Conference on Unmanned Aircraft Systems (ICUAS)*, pp. 1106-1113, 2023, <https://doi.org/10.1109/ICUAS57906.2023.10156505>.
- [6] T. Susanto, M. Bayu Setiawan, A. Jayadi, F. Rossi, A. Hamdhi and J. Persada Sembiring, "Application of Unmanned Aircraft PID Control System for Roll, Pitch and Yaw Stability on Fixed Wings," *2021 International Conference on Computer Science, Information Technology, and Electrical Engineering (ICOMITEE)*, pp. 186-190, 2021, <https://doi.org/10.1109/ICOMITEE53461.2021.9650314>.
- [7] M. Esfandiari and M. A. Amiri Atashgah, "Reinforcement Learning Control of an Aerial Robot Based on a Tuned Proximal Policy Optimization in Takeoff and Hover Phases," *2022 10th RSI International Conference on Robotics and Mechatronics (ICRoM)*, pp. 165-171, 2022, <https://doi.org/10.1109/ICRoM57054.2022.10025140>.
- [8] V. P. Tran, F. Santoso, M. A. Garratt and I. R. Petersen, "Distributed Formation Control Using Fuzzy Self-Tuning of Strictly Negative Imaginary Consensus Controllers in Aerial Robotics," in *IEEE/ASME*

- Transactions on Mechatronics*, vol. 26, no. 5, pp. 2306-2315, 2021, <https://doi.org/10.1109/TMECH.2020.3036829>.
- [9] M. Mazinani, P. Zarafshan, M. Dehghani, H. Etezadi, K. Vahdati and G. Chegini, "Modeling and Control of a Pollinator Flying Robot," *2021 9th RSI International Conference on Robotics and Mechatronics (ICRoM)*, pp. 548-553, 2021, <https://doi.org/10.1109/ICRoM54204.2021.9663526>.
- [10] A. S. Priambodo, F. Arifin, A. Nasuha, A. Winursito, "Face Tracking for Flying Robot Quadcopter based on Haar Cascade Classifier and PID Controller," *Journal of Physics: Conference Series*, vol. 2111, no. 1, p. 012046, 2021, <https://doi.org/10.1088/1742-6596/2111/1/012046>.
- [11] I. Trenev, A. Tkachenko, A. Kustov, "Movement stabilization of the parrot mambo quadcopter along a given trajectory based on PID controllers," *IFAC-PapersOnLine*, vol. 54, no. 13, pp. 227-232, 2021, <https://doi.org/10.1016/j.ifacol.2021.10.450>.
- [12] J. Mou, W. Zhang, K. Zheng, Y. Wang, C. Wu, "More detailed disturbance measurement and active disturbance rejection altitude control for a flapping wing robot under internal and external disturbances," *Journal of Bionic Engineering*, vol. 19, no. 6, 1722-1735, 2022, <https://doi.org/10.1007/s42235-022-00236-7>.
- [13] A. Baba, B. Alothman, "A fuzzy logic-based stabilization system for a flying robot, with an embedded energy harvester and a visual decision-making system," *Robotics and Autonomous Systems*, pp. 104471, 2023, <https://doi.org/10.1016/j.robot.2023.104471>.
- [14] M. Maier, M. Keppler, C. Ott and A. Albu-Schäffer, "Adaptive Air Density Estimation for Precise Tracking Control and Accurate External Wrench Observation for Flying Robots," *IEEE Robotics and Automation Letters*, vol. 5, no. 2, pp. 1445-1452, 2020, <https://doi.org/10.1109/LRA.2020.2967333>.
- [15] M. Taherinezhad, A. Ramirez-Serrano, and A. Abedini, "Robust Trajectory-Tracking for a Bi-Copter Drone Using INDI: A Gain Tuning Multi-Objective Approach," *Robotics*, vol. 11, no. 5, p. 86, 2022, <http://dx.doi.org/10.3390/robotics11050086>.
- [16] M. Pimentel and M. Basiri, "A Bimodal Rolling-Flying Robot for Micro Level Inspection of Flat and Inclined Surfaces," in *IEEE Robotics and Automation Letters*, vol. 7, no. 2, pp. 5135-5142, 2022, <https://doi.org/10.1109/LRA.2022.3154027>.
- [17] A. H. C. Abantas, W. A. Sabellona and C. J. O. Salaan, "Design of a Rule-Based Tuned PID Controller for Tether Management of a Suspended Tethered UAV," *2022 IEEE 14th International Conference on Humanoid, Nanotechnology, Information Technology, Communication and Control, Environment, and Management (HNICEM)*, pp. 1-6, 2022, <https://doi.org/10.1109/HNICEM57413.2022.10109555>.
- [18] D. Baidya, S. Dhopte and M. Bhattacharjee, "Sensing System Assisted Novel PID Controller for Efficient Speed Control of DC Motors in Electric Vehicles," *IEEE Sensors Letters*, vol. 7, no. 1, pp. 1-4, 2023, <https://doi.org/10.1109/LSSENS.2023.3234400>.
- [19] A. Khalil, M. A. Jaradat, S. Mukhopadhyay and M. F. Abdel-Hafez, "Autonomous Control of a Hybrid Rolling and Flying Caged Drone for Leak Detection in HVAC Ducts," *IEEE/ASME Transactions on Mechatronics*, pp. 1-13, 2023, <https://doi.org/10.1109/TMECH.2023.3279870>.
- [20] D. Horla, W. Giernacki, T. Báča, V. Spurny, M. Saska, "AL-TUNE: A family of methods to effectively tune UAV controllers in in-flight conditions," *Journal of Intelligent & Robotic Systems*, vol. 103, no. 5, 2021, <https://doi.org/10.1007/s10846-021-01441-y>.